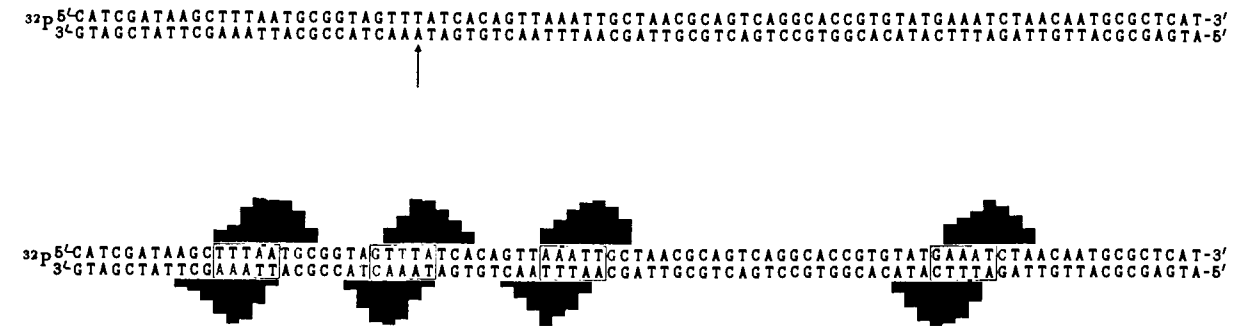

Figure 3. Base pairs 22-108 from pBR322 plasmid.[15] (Top) Arrow indicates major site of DNA cleavage[14] resulting from reaction with BD on 167-bp restriction fragment after 5 and 10 h at 37 °C (pH 7.0). (Bottom) MPE·Fe^{II} footprints of BD at 5 μM concentration bound to 167 bp restriction fragment at 37 °C (pH 7.0). Asymmetric histograms on each strand represent regions on the 5′ (and 3′) ^{32}P end-labeled DNA restriction fragment protected by BD from cleavage by MPE·Fe^{II} (Fig. 2, lanes 9, 10). Boxes are equilibrium binding sites of BD whose assignment is based on the MPE·Fe^{II} footprinting model described in ref 6b,c and 7.

sites at 5 μM concentration on the 167 bp fragment (5′-3′) TTTAA, GTTTA, AAATT, and GAAAT (Figure 3). These are the same sites bound by distamycin.[7,8] The major cleavage site is contained within one of these four equilibrium binding sites on the complementary strand of the 5′-GTTTA-3′ site as shown by the arrow in Figure 3.[14] At reaction times longer than 10 h a second cleavage site becomes visible at the first adenine in the binding site, 5′-AAATT-3′.

An understanding of the mechanistic details by which the synthetic BD exhibits preferential cleavage at one of 334 nucleotides in the 167-bp DNA fragment[14] must await characterization of the DNA cleavage products[16] and kinetic analyses. From the MPE·Fe^{II} footprinting results at 37 °C (0.5 h), we find that the *N*-bromoacetyl moiety has not changed significantly the equilibrium binding specificity of the tripeptide unit on DNA because we observe the same DNA binding sites for BD as the natural product distamycin. The few cleavage sites observed at 37 °C (5-10 h) may indicate unequal relative rates of reaction of a minimum of seven adenines proximal to the bound bromoacetyltripeptide within the four tripeptide equilibrium binding sites. If this is true, the different rates of reaction at proximal adenines may be a reflection of the sequence-dependent differences of local structure of B-form DNA[9] and the stereoelectronic requirement in the transition state for the backside nucleophilic displacement reaction. In fact, the synthetic bromoacetyldistamycin may mimic in mechanistic aspects the natural product antitumor agent CC-1065 which alkylates DNA at A·T rich regions five base pairs in size.[2]

Finally, we had previously reported that tris(*N*-methylpyrrolecarboxamide) equipped with EDTA·Fe^{II}[distamycin-EDTA·Fe^{II}] affords multiple cleavage patterns flanking both sides of a five-base-pair A·T rich binding site.[8] Because the bromoacetyl moiety is nondiffusible, the electrophilic-mediated cleavage affords single cleavage events within each equilibrium binding site which can be distinguished from the multiple cleavage loci caused by a diffusible oxidant generated by EDTA·Fe^{II}. By changing the DNA cleaving function attached to the same DNA binding unit [tris(*N*-methylpyrrolecarboxamide)], from a *non-sequence-specific diffusible* oxidant to a *sequence-specific nondiffusible* electrophile, we find quite different levels of sequence-specific DNA cleavage. From the point of view of determining the sequence specificity of DNA binding molecules, the nonspecific DNA cleaving function EDTA·Fe^{II} is preferred.[17] From the point of view of designing a very specific DNA cleaving molecule, the combination of a base-specific DNA cleaving moiety with a sequence-specific DNA binding unit affords a highly discriminating DNA cleaving molecule.

Acknowledgment. We are grateful to the National Institutes of Health (GM-27681) for support of this research.

(16) The DNA termini at the cleavage site are 5′-phosphate and 3′-phosphate. This is consistent with alkylation of adenine followed by depurination and deoxyribose hydrolysis to afford a "gap" at the cleavage site.

(17) The affinity cleaving technique simply takes advantage of the analytical power of high-resolution denaturing gel electrophoresis to determine the sequence specificities of equilibrium binding molecules on DNA.[8]

NMR Evidence for a Horseradish Peroxidase State with a Deprotonated Proximal Histidine

Jeffrey S. de Ropp,[1b] V. Thanabal,[1a] and Gerd N. La Mar*[1a]

Department of Chemistry and UCD NMR Facility
University of California, Davis, California 95616
Received July 22, 1985

The modulation of heme iron reactivity in peroxidases by removal of the labile proton from the ubiquitous proximal histidine has long been postulated.[2-5] Both resonance Raman and electronic spectra of reduced horseradish peroxidase (HRP) have been interpreted in terms of a deprotonated proximal imidazole.[6-9] However, for both reduced- and resting-state HRP, the presence of this proton could be established in the ^1H NMR spectrum by its characteristic large downfield hyperfine shift,[10-12] as found in model compounds,[13] confirming the presence of an imidazole rather than an imidazolate as axial ligand in the five-coordinate state. Both functional states of HRP,[2,5] the enzymatic intermediates HRP compounds I and II, however, are six-coordinate, and little is known about the nature of the axial imidazole in such low-spin derivatives. While the relevant resonance Raman bands, to our knowledge, have not been located in any low-spin six-coordinate HRP complex, some indirect NMR data[14] on nonexchangeable protons have suggested extensive imidazolate character in the cyano complex HRPCN. Labile proton signals consistent with originating from the axial histidyl imidazole have been re-

(1) (a) Department of Chemistry. (b) UCD NMR Facility.
(2) Morrison, M.; Schonbaum, G. R. *Annu. Rev. Biochem.* **1976**, *45*, 861-888.
(3) Nicholls, P. *Biochim. Biophys. Acta* **1962**, *60*, 217-228.
(4) Blumberg, W. E.; Peisach, J. In "Probes of Structure and Function of Macromolecules and Membranes"; Chance, B., Yonetani, T., Mildvan, A. S., Eds.; Academic Press: New York, 1971; Vol. II, pp 215-229.
(5) Schonbaum, G. R. In "Oxidases and Related Redox Systems"; King, E., Mason, H, S., Morrison, M., Eds.; Pergamon Press: Oxford, 1982; pp 671-684.
(6) Stein, P.; Mitchell, M.; Spiro, T. G. *J. Am. Chem. Soc.* **1980**, *102*, 7795-7797.
(7) Teraoka, J.; Kitagawa, T. *J. Biol. Chem.* **1981**, *256*, 3969-3977.
(8) Desbois, A.; Mazza, G.; Stretzkowski, F.; Lutz, M. *Biochim. Biophys. Acta* **1984**, *785*, 161-176.
(9) Mincey, T.; Traylor, T. G. *J. Am. Chem. Soc.* **1979**, *101*, 765-766.
(10) La Mar, G. N.; de Ropp, J. S. *Biochem. Biophys. Res. Commun.* **1979**, *90*, 36-41.
(11) La Mar, G. N.; de Ropp, J. S. *J. Am. Chem. Soc.* **1982**, *104*, 5203-5206.
(12) La Mar, G. N.; de Ropp, J. S.; Smith, K. M.; Langry, K. C. *J. Biol. Chem.* **1980**, *255*, 6646-6652.
(13) La Mar, G. N.; Budd, D. L.; Goff, H. *Biochem. Biophys. Res. Commun.* **1977**, *77*, 104-110.
(14) La Mar, G. N.; de Ropp, J. S.; Chacko, V. P.; Satterlee, J. D.; Erman, J. E. *Biochim. Biophys. Acta* **1982**, *708*, 317-325.

0002-7863/85/1507-8268$01.50/0

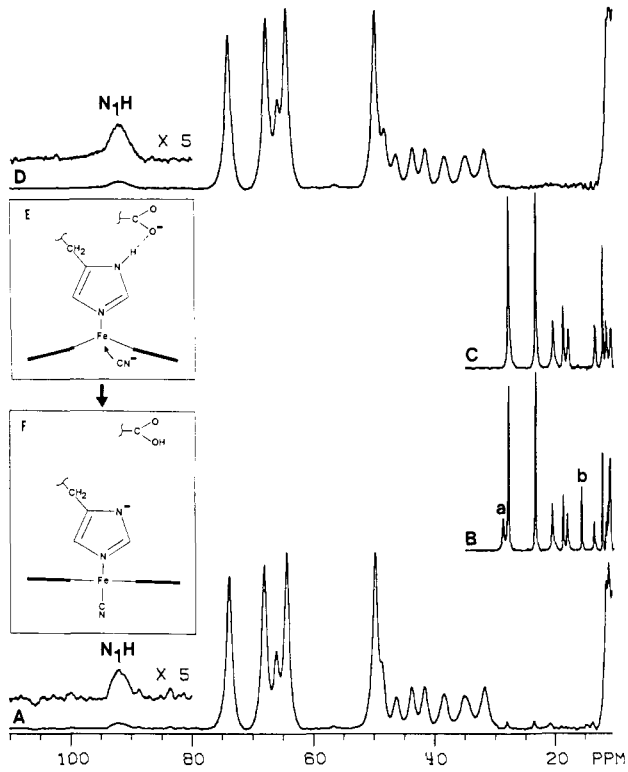

Figure 1. Downfield portions of the 360-MHz ^1H hyperfine shifted spectra at pH 7.0, 55 °C, of (A) resting-state HRP freshly dissolved in ^2H_2O, (B) HRPCN in 90% H_2O/10% ^2H_2O, (C) HRPCN formed by treatment of sample shown in trace (A) with 2 equiv of KCN, and (D) resting-state HRP reformed by treatment of sample shown in trace C with ten equivalents of hydroxocobalamine hydrochloride. Traces (A) and (D) show the proximal N_1H resonance; trace (B) shows exchangeable resonances a and b. Schematic representation of (E) five-coordinate high-spin hemin in resting-state HRP and (F) six-coordinate low-spin hemin in HRPCN. (E) shows the pentacoordinate iron in the expected domed configuration with significant out-of-plane displacement toward the proximal histidine. The postulated hydrogen-bonding interaction between the histidyl ring NH and an amino acid acceptor is shown severed in (F) as the cyanide ligation pulls the iron in plane with concomitant flattening of the porphyrin resulting in the breaking of the histidyl ring NH–carboxylate hydrogen bond, generating a proximal histidyl imidazolate in HRPCN. The tight clamping of the heme by the amino acids in the heme pocket prevents the porphyrin from changing position.

ported,[15] but unambiguous assignment has not been possible. We report herein on ^1H NMR studies of HRPCN which provide direct evidence that the proximal histidyl imidazole is indeed deprotonated and that the proton transfer is to a site shielded from bulk solvent in the protein interior.

The determination that the proximal histidine is deprotonated in HRPCN relies on both the previous unambiguous assignment and known exchange rate for the proximal histidyl imidazole labile proton in resting state HRP,[10] a knowledge of the possible resonance position of this proton in low-spin ferric derivatives if they possess a neutral imidazole,[16-18] and the facility to interconvert the two states, HRP and HRPCN, by use of appropriate reagents (vide infra). In high-spin ferric HRP, the imidazole ring NH signal is clearly detected, even upon dissolution in ^2H_2O, as shown in A of Figure 1; the exchange lifetime is ~4 h at 55 °C.[19] This proton, if present in HRPCN, must resonate downfield of its diamagnetic position at ~12 ppm because of a necessarily downfield dipolar shift dictated by the characteristic magnetic anisotropy of low-spin hemin.[20] Thus the ring NH is expected to resonate in the window downfield of 12 ppm and is found at 15–25 ppm in a variety of model complexes[16-18] as well as protein derivatives.[21-23] HRPCN dissolved in H_2O shows two exchangeable resonances downfield of 12 ppm, designated a and b in Figure 1B. Peak a resonates at the appropriate position and has the characteristic relaxation properties (paramagnetic contribution to the linewidth ca. 3 times that of a heme methyl) for the proximal N_1H. However, both peaks a and b have rapid exchange rates (>1 s^{-1}) with bulk solvent, since very rapid dissolution of HRPCN in ^2H_2O (within 2 min) fails to yield detectable signals at the positions of a and b (trace C in Figure 1).

The great disparity in rate of exchange of the hyperfine-shifted labile peaks between resting state HRP and HRPCN provided the framework for the following experiment. Resting state HRP was dissolved in ^2H_2O and the spectrum recorded showing the characteristic unit intensity proximal N_1H resonance as is shown in A of Figure 1. Under these conditions the proton is detectable for several hours. When cyanide is added to convert the protein to HRPCN, the NMR trace is as shown in C of Figure 1, failing to reveal *any* labile hyperfine-shifted resonances. Of particular interest here, there is no exchangeable resonance at a shift ≥12 ppm. However, when the cyanide in this sample is removed after 20 min (by adding hydroxocobalamine hydrochloride whose significantly greater affinity for cyanide strips the ligand from the protein within a few seconds), the resulting resting state HRP spectrum still reveals the N_1H peak at 92 ppm (Figure 1D). Thus the axial ring NH has approximately as low a lability in HRPCN as in resting-state HRP. This establishes two facts: first, that neither a nor b in the spectrum of HRPCN can arise from the proximal N_1H. Second, the rate of exchange of the (unobserved) proximal N_1H of the HRPCN form is sufficiently long so that it cannot experience detectable lifetime broadening of its signal. Thus this proton must give a resolvable signal in the region downfield of 12 ppm if it is attached to the histidyl imidazole ring. The absence of such a labile proton signal in HRPCN in H_2O in the temperature range 5–55 °C[24] (Figure 1B) dictates that the NH imidazole ring is deprotonated and the proton transferred to a localized acceptor site at some distance from the iron-bound imidazolate and resonating in the diamagnetic envelope 0–10 ppm. We therefore must conclude that the addition of cyanide to resting-state HRP to form HRPCN is accompanied by a transfer of the imidazole labile proton to an amino acid. The dynamic stability of the proximal side of the heme pocket is confirmed by the localized nature of the transfer in that no exchange with bulk water takes place.

The proton transfer from the imidazole in HRPCN can be rationalized on the basis of the known stereochemistry of heme iron.[25] The X-ray structure of cytochrome *c* peroxidase, CcP,[26,27]

(15) La Mar, G. N.; Chacko, V. P.; de Ropp, J. S. In "The Biological Chemistry of Iron"; Dunford, H. B., Dolphin D., Raymond, K., Sieber, L., Eds.; D. Reidel Publishing Co.: Boston, 1982; pp 357–373.
(16) Satterlee, J. D.; La Mar, G. N. *J. Am. Chem. Soc.* **1976**, *98*, 2804–2808.
(17) La Mar, G. N.; Frye, J. S.; Satterlee, J. D. *Biochim. Biophys. Acta* **1976**, *428*, 78–90.
(18) Chacko, V. P.; La Mar, G. N. *J. Am. Chem. Soc.* **1982**, *104*, 7002–7007.
(19) de Ropp, J. S. Ph.D. Thesis, University of California, Davis, 1981.
(20) In resting-state HRP the origin of hyperfine shifts is predominantly contact (through-bond) due to the largely isotropic iron ferric high-spin state. In contrast, ferric low-spin iron is highly anisotropic, giving rise to large dipolar shifts. For protons above the heme plane and the iron the geometric dependence of the dipolar shift produces downfield shifts for these sites. Though the contact shift for the imidazole ring NH is upfield, it is smaller in magnitude than the downfield dipolar shift resulting in the expected shift downfield of the diamagnetic reference. Any lessening of the NH bonding due to hydrogen bonding to an amino acid acceptor must decrease the contact shift resulting in larger downfield shift due to the dipolar term if all other parameters are constant. Only if the proton were removed from the histidyl imidazole ring would the resonance be in the diamagnetic envelope 0–10 ppm. Thus the hyperfine dipolar shift moves the proximal N_1H further downfield than its diamagnetic position of ~12 ppm.
(21) Ogawa, S.; Shulman, R. G.; Yamane, T. *J. Mol. Biol.* **1972**, *70*, 291–300.
(22) Cutnell, J. D.; La Mar, G. N.; Kong, S. B. *J. Am. Chem. Soc.* **1981**, *103*, 3567–3572.
(23) Kong, S. B.; Cutnell, J. D.; La Mar, G. N. *J. Biol. Chem.* **1983**, *258*, 3843–3849.
(24) No slowly exchanging peak was detected outside the diamagnetic envelope of resonances 0–10 ppm over the temperature range of 5–55 °C.
(25) Scheidt, W. R.; Reed, C. A. *Chem. Rev.* **1981**, *81*, 543–555.

has identified a strong proton acceptor (Asp-235) near the axial imidazole ring NH, which, due to sequence homology in this region between CcP[28] and HRP,[29] is likely similarly situated in resting-state HRP, as depicted in Figure 1E. Since resting-state HRP is five-coordinate,[12] we assume the characteristic domed porphyrin and a sizable out-of-plane displacement of the iron[25] such that the imidazole ring NH can interact with the carboxylate. Upon coordination of cyanide, the conversion to low-spin iron flattens the porphyrin and brings the iron into the plane.[25] Because of the tight clamping of the heme periphery,[30] this resulting 0.5-1.0-Å movement of the imidazole ring breaks the salt bridge to the amino acid, with the proton retained by the carboxylate rather than the imidazole ring, as depicted in Figure 1F. Thus the six-coordinate compounds I and II, but not five-coordinate resting-state HRP, may possess the axial imidazolate to stabilize the higher oxidation state of iron.

Nuclear Overhauser effect studies of the rapidly exchanging peaks a and b of HRPCN in H_2O (not shown) reveal that the two peaks are in spatial proximity and are consistent with arising from a histidine in the distal environment of the heme, for which strong interaction with a coordinated ligand has been demonstrated by IR spectroscopy.[31] Further definitive assignments of the labile proton signals are in progress.

Acknowledgment. This work was supported by the National Institutes of Health, Grant GM-26226. We gratefully acknowledge the procedure of hydroxocobalamine hydrochloride strip of cyanide suggested to us by M. F. Perutz.

Registry No. HRP, 9003-99-0; Fe, 7439-89-6; histidine, 71-00-1; cyanide, 57-12-5.

(26) Poulos, T. L.; Kraut, J. *J. Biol. Chem.* **1980**, *255*, 8199-8205.
(27) Finzel, B. C.; Poulos, T. L.; Kraut, J. *J. Biol. Chem.* **1984**, *259*, 13027-13036.
(28) Takio, K.; Titani, K.; Ericsson, L. H.; Yonetani, T. *Arch. Biochem. Biophys.* **1980**, *203*, 615-629.
(29) Welinder, K. G. *Eur. J. Biochem.* **1979**, *96*, 483-502.
(30) La Mar, G. N.; de Ropp, J. S.; Smith, K. M.; Langry, K. C. *J. Am. Chem. Soc.* **1983**, *105*, 4576-4580.
(31) Smith, M. L.; Ohlsson, P.-I.; Paul, K. G. *FEBS Lett.* **1983**, *163*, 303-305.

Metal-Metal Bonds Involving Actinides. Synthesis and Characterization of a Complex Having an Unsupported Actinide to Transition-Metal Bond

Richard S. Sternal, Carolyn P. Brock, and Tobin J. Marks*

Department of Chemistry, Northwestern University Evanston, Illinois 60201

Received August 22, 1985

While metal-metal bonding is a ubiquitous feature of transition-metal chemistry and heterobimetallic ("early-late") systems are of considerable current interest,[1,2] no well-characterized example of an actinide to transition-metal bond unsupported/uncomplicated by bridging ligands[3] exists. The competing formation of isocarbonyl linkages (A)[1a,4] between highly oxophilic 5f centers[5]

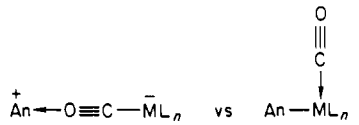

An = actinide; M = transition metal

and metal carbonyl synthons has been a major obstacle,[6] and in our view, strategies to promote B must minimize crowding around the An-ML_n(CO) bond and/or provide an ML_n(CO) fragment with an appropriately directed, high-lying, metal-centered HOMO. Using ML_n(CO) = $CpRu(CO)_2$[2a-d,7] and An = $Cp'_2Th(X)$ (Cp = η^5-C_5H_5; Cp' = η^5-$(CH_3)_5C_5$) as prototypes in this strategy, we report the synthesis and structural characterization of the first complexes with *direct, unsupported*, actinide to transition-metal bonds.

The reaction of Cp'_2ThX_2 (X = Cl,[8] I[9]) with $CpRu(CO)_2Na$[10]

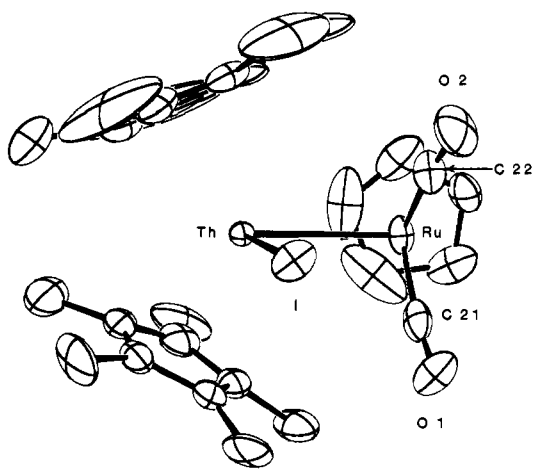

Figure 1. Perspective drawing of the molecular structure of $Cp'_2Th(I)$-$Ru(Cp)(CO)_2$ (**2**). The shapes of the ellipsoids correspond to 50% probability contours of atomic displacement. Individual bond lengths (Å) and angles (deg) of interest: Th-Ru, 3.0277 (6); Th-I, 3.0435 (6); Th-C (Cp' ring), 2.82 (1, 2, 4, 10);[13b] Ru-C21, 1.88 (2); Ru-C22, 1.84 (1); Ru-C(Cp ring), 2.29 (1, 1, 2, 5);[13b] Th-Ru-C21, 83.8 (2); Th-Ru-C22, 84.4 (3); C21-Ru-C22, 88.3 (5); Th-Ru-Cp centroid, 118.4.

(1) (a) Edidin, R. T.; Longato, B.; Martin, B. D.; Matchett, S. A.; Norton, J. R. In "Organometallic Compounds"; Shapiro, B. L.; Ed.; Texas A&M University Press: College Station, TX, 1983; pp 260-280 and references therein. (b) Roberts, D. A.; Geoffroy, G. L. In "Comprehensive Organometallic Chemistry"; Wilkinson, G.; Stone, F. G. A.; Abel, E. W., Eds.; Pergamon Press: Oxford, 1982; Vol. 6, Chapter 40. (c) Masters, C. *Adv. Organomet. Chem.* **1979**, *17*, 61-103.
(2) (a) Casey, C. P.; Jordon, R. F.; Rheingold, A. L. *J. Am. Chem. Soc.* **1983**, *105*, 665-667. (b) Casey, C. P.; Jordon, R. F.; Rheingold, A. L. *Organometallics* **1984**, *3*, 504-506. (c) Casey, C. P.; Palermo, R. E.; Jordon, R. F.; Rheingold, A. L. *J. Am. Chem. Soc.* **1985**, *107*, 4597-4599. (d) Sartain, W. J.; Selegue, J. P. *J. Am. Chem. Soc.* **1985**, *107*, 5818-5820. (e) Barger, P. T.; Bercaw, J. E. *Organometallics* **1984**, *3*, 278-284.
(3) In phosphido-bridged systems, relatively close actinide-transition-metal contacts are thought to reflect some degree of transition-metal → thorium dative bonding: (a) Ritchey, J. M.; Zozulin, A. J.; Wrobleski, D. A.; Ryan, R. R.; Wasserman, H. J.; Moody, D. C.; Paine, R. T. *J. Am. Chem. Soc.* **1985**, *107*, 501-503. (b) Hay, P. J.; Ryan, R. R.; Salazar, K. V.; Wrobleski, D. A.; Sattelberger, A. P. *J. Am. Chem. Soc.*, submitted for publication. (c) Ortiz, J. V., submitted for publication. We thank these authors for preprints.
(4) (a) Darensbourg, M. Y. *Prog. Inorg. Chem.* **1985**, *33*, 221-274. (b) Horwitz, C. P.; Shriver, D. F. *Adv. Organomet. Chem.* **1984**, *23*, 219-305. (c) Boncella, J. M.; Andersen, R. A. *Inorg. Chem.* **1984**, *23*, 432-437 and references therein. (d) Merola, J. S.; Campo, K. S.; Gentile, R. A.; Modrick, M. A.; Zentz, S. *Organometallics* **1984**, *3*, 334-337 and references therein. (e) Marsella, J. A.; Huffman, J. C.; Caulton, K. G.; Longato, B.; Norton, J. R. *J. Am. Chem. Soc.* **1982**, *104*, 6360-6368 and references therein. (f) Hamilton, D. M., Jr.; Willis, W. S.; Stucky, G. D. *J. Am. Chem. Soc.* **1981**, *103*, 4255-4256. (g) Onaka, S.; Furuichi, N. *J. Organometal. Chem.* **1979**, *173*, 77-88. (h) Crease, A. E.; Legzdins, P. *J. Chem. Soc., Dalton Trans.* **1973**, 1501-1507.
(5) (a) Marks, T. J.; Fragalà, I. L., Eds. "Fundamental and Technological Aspects of Organo-f-Element Chemistry"; Reidel: Dordrecht 1985. (b) Marks, T. J.; Ernst, R. D. In ref 1b, Vol. 3, Chapter 21.
(6) (a) Marks, T. J., unpublished results. (b) Bennett, R. L.; Bruce, M. I.; Stone, F. G. A. *J. Organomet. Chem.* **1971**, *26*, 355-356. (c) Fagan, P. J.; Mintz, E. A.; Marks, T. J., unpublished results on $Cp_2U[Mo(Cp(CO)_3]_2$ quoted in ref 5b, p 261. (d) Dormand, A.; Moise, C. *Polyhedron* **1985**, *4*, 595-598.
(7) Electronic structure studies on related fragments: (a) Bursten, B. E.; Gatter, M. G. *J. Am. Chem. Soc.* **1984**, *106*, 2554-2558. (b) Schilling, B. E. R.; Hoffmann, R.; Lichtenberger, D. L. *J. Am. Chem. Soc.* **1979**, *101*, 585-591.
(8) Fagan, P. J.; Manriquez, J. M.; Maatta, E. A.; Seyam, A. M.; Marks, T. J. *J. Am. Chem. Soc.* **1981**, *103*, 6650-6667.

0002-7863/85/1507-8270$01.50/0